Pyridine versus Acetonitrile Coordination in Rhodium–N-Heterocyclic Carbene Square-Planar Complexes

Laura Palacios,[‡] Andrea Di Giuseppe,[‡] Ricardo Castarlenas,*[,‡] Fernando J. Lahoz,[‡] Jesús J. Pérez-Torrente,[‡] Luis A. Oro[‡,†]

Experimental and theoretical studies on the factors that control the coordination chemistry of N-donor ligands in square-planar complexes of type RhCl(NHC)L^1L^2 (NHC = N-heterocyclic carbene) are presented. The dinuclear complexes [Rh(μ-Cl)(IPr)(η^2-olefin)]$_2$ {IPr = 1,3-bis-(2,6-diisopropylphenyl)imidazol-2-carbene}, have been reacted with different combinations of ligands including pyridine, acetonitrile, 2-pyridylacetonitrile, triphenylphosphine, tricyclohexylphosphine, carbon monoxide or molecular oxygen. In addition, the reactivity of RhCl(IPr)(PPh_3)$_2$ has also been studied. Pyridine preferentially coordinates *trans* to the carbene ligand whereas π-acceptor ligands (olefin, CO or PPh_3) are prone to bind *cis* to IPr and *trans* to chlorido, unless steric bulk hinders the coordination of the ligand (PCy_3). In contrast, acetonitrile is more labile than pyridine but it is able to form complexes coordinated *cis*-to IPr. Molecular dioxygen also displaces the labile cyclooctene ligand in RhCl(IPr)(η^2-coe)(py) to give a square planar dioxygen adduct which can be transformed into a peroxo derivative by additional coordination of pyridine. Charge Decomposition Analysis (CDA) shows that σ-donation values are similar for coordination at *cis*- or *trans*-IPr positions, whereas efficient π-backbonding is significantly observed at *cis* position being the favoured coordination site for π-acceptor ligands. The Rh-IPr rotational barrier in a series of square-planar complexes has been analysed. It has been found that main contribution is the steric hindrance of the ancillary ligand. The presence of a π-donor ligand such as chlorido slows down the dynamic process.

Introduction

Catalytic efficiency for a specific transition-metal mediated transformation requires the appropriate choice of a particular set of ligands that determine the catalytic outcome.[1] Therefore, a detailed study of coordination chemistry within intermediate species is essential in order to a rational design of active and selective catalysts.[2] Commonly, organometallic catalysts bear a primary ligand, such as cyclopentadienyl, phosphine, alkylidene, porphyrin, salen, etc, that accounts for the main catalytic properties, whereas ancillary ligands or additives frequently tune the activity or selectivity in a subtle way. This principal ligand may, in certain cases, modulate the position and tightness of ancillary ligands and substrates, thus exerting critical influence over the catalytic results. N-heterocyclic carbenes (NHCs)[3] belong to this class of ligands due to their particular donor-acceptor properties[4] and high steric hindrance[5] (Chart 1).

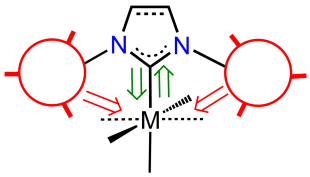

Chart 1. Steric and electronic influence of NHC ligands.

An outstanding example of this NHC ligand-management effect has been recently discovered in our laboratories.[6] Addition of pyridine to the alkyne hydrothiolation[7] catalysts [Rh(μ-Cl)(NHC)(η^2-olefin)]$_2$, dramatically switches the regioselectivity to the formation of branched vinyl sulfides. It has been demonstrated that pyridine coordination *trans* to the NHC ligand in the key hydride-thiolate catalytic intermediate species, directs the coordination of the alkyne *cis* to the carbene ligand. The higher *trans-influence* of the hydride ligand paves the way to a *cis* thiolate-alkyne disposition, thereby favouring thiolate insertion. It has been found that subtle modifications on the pyridine motif significantly accounts for the selectivity, similar to other pyridine-modulated catalytic transformations.[8] In contrast, the addition of other typical N-donor additives such as acetonitrile do not affect the selectivity as much as pyridine does,[9] more likely due to the different coordination capability. Particularly for M-NHC complexes, a clear trend in favour of one of such nitrogenated ligands is not observed and competitive coordination of acetonitrile[10] or pyridine[11] depends on a complex interplay between electronic and steric factors. Prompted by these precedents, we present herein an experimental and theoretical study of the coordination of different N-donor ligands into Rh-NHC square-planar complexes.

Results and Discussion

Synthesis of pyridine and acetonitrile complexes

Dinuclear olefin complexes [Rh(μ-Cl)(IPr)(η^2-olefin)]$_2$ {olefin = coe (cyclooctene) (**1**), ethylene (**2**)} {IPr = 1,3-bis-(2,6-diisopropylphenyl)imidazol-2-carbene} are adequate precursors for the preparation of a wide array of mononuclear complexes bearing varied ligands.[12] As shown previously in our group, pyridine (py) ligands are able to cleave the chlorido-bridges of **1** and **2** to generate mononuclear complexes of type RhCl(IPr)(η^2-olefin)(py) {coe (**3a**), ethylene (**3b**)}, although the η^2-olefin was not exchanged even on heating **1** in neat pyridine at 80 ºC for one night.[6] Now, we have observed that acetonitrile behaves differently. Unexpectedly, the starting materials were recovered unreacted after stirring at room temperature for 3 h a solution of **1** or **2** in a mixture toluene (2 mL) / acetonitrile (2 mL). However, *in-situ* treatment of toluene-d_8 samples of **1** and **2** on an NMR tube scale with an excess of acetonitrile (100 μL) showed the presence of two different species depending on the coordinated olefin. In the case of ethylene, the new resonances were ascribed to RhCl(IPr)(η^2-CH_2=CH_2)(CH_3CN) (**4**), resulting from acetonitrile cleavage of the chlorido-bridges of **2**. Complex **4** likely reverts to the dinuclear species **2** during the isolation process (Scheme 1).[13] The ^{1}H NMR spectrum of **4** at -20 ºC showed two doublets at δ 2.47 and 2.33 ppm (J_{H-H} = 12.3 Hz) for the η^2-olefinic protons and a singlet at 2.15 ppm corresponding to the coordinated acetonitrile molecule. The spectrum at room temperature showed a broadening of ethylene and IPr signals indicating a rotational process for both ligands, but unfortunately the activation parameters could not be determined.[12h] The more noticeable signals in the ^{13}C{^{1}H}-APT NMR spectrum are two doublets at δ 181.4 ppm (J_{C-Rh} = 56.7 Hz) and 41.8 ppm (J_{C-Rh} = 15.4 Hz) corresponding to the IPr and ethylene ligands. In contrast, addition of acetonitrile to the η^2-coe derivative **1** at room temperature gave rise to a new set of signals that grew up after heating at 80º C for 5 h with concomitant appearance of free coe. The new complex was isolated and characterized as the cationic derivative [Rh(IPr)(CH_3CN)$_3$]Cl (**5**), in which not only coe but chlorido ligands have been replaced by acetonitrile (Scheme 1). The structure of **5** was unequivocally unravelled by comparison of the ^{1}H and ^{13}C{^{1}H} NMR spectra with those of the triflate salt, [Rh(IPr)(CH_3CN)$_3$]OTf, that has been recently prepared by protonation of Rh(acac)(IPr)(coe) (acac = acetylacetonate) with triflic acid.[12h] Interestingly, compound **5** was not obtained on heating a solution of an equilibrium mixture of **2** and **4** in CD_3CN at 80 ºC for 5 h, which demonstrates the different bond strength of ethylene and coe.[14] Prolonged reaction times led to decomposition of the sample.

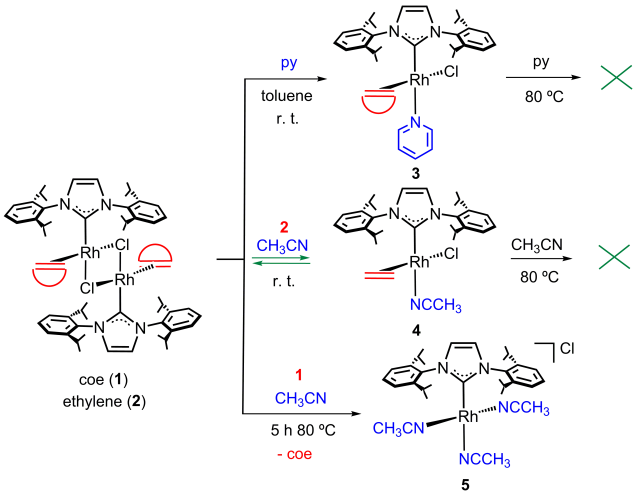

Scheme 1. Bridge-cleavage reactions promoted by N-donor ligands.

DFT calculations on the thermodynamic equilibrium for the exchange reaction between olefin and N-donor ligands in **3** and **4** were performed (Scheme 2). In accordance with the experimental results, we have found that the formation of putative disubstituted N-donor ligand complexes RhCl(IPr)(py)$_2$ (**6t**) and RhCl(IPr)(CH_3CN)$_2$ (**7t**) is disfavoured by an average of 16.4 (coe) and 13.0 (ethylene) kcal mol^{-1}. Certainly, the higher π-acceptor capacity of the olefin with regard to pyridine or acetonitrile may be determinant in the stability of these electron-rich Rh^{I} derivatives.

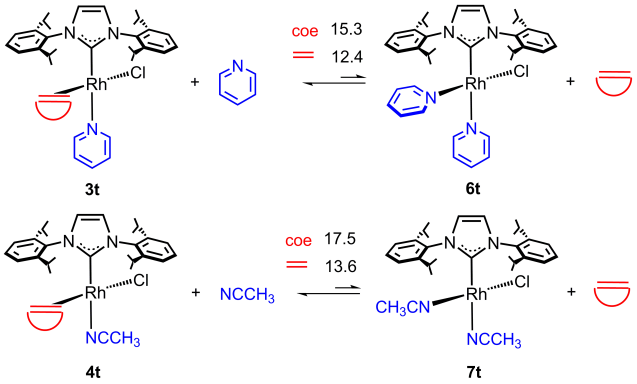

Scheme 2. DFT calculated ΔE (kcal mol^{-1}) for the thermodynamic equilibrium between coordinated olefin and pyridine or acetonitrile.

In order to further compare the pyridine and acetonitrile coordination capabilities, complexes **1** and **2** were treated with 2-pyridylacetonitrile. At room temperature, the chloride-bridges were cleaved to give rise to the mononuclear complexes RhCl(IPr)(η^2-olefin){κ-*N*,(NC$_5$H$_4$)-2-CH_2CN} {coe = (**8**); ethylene (**9**)}, bearing the pyridine moiety coordinated to the metal center and a free nitrile group (Scheme 3). No chelate or dinuclear species were observed. Coordination of a second equivalent of 2-pyridylacetonitrile was observed on heating **8** at 80 ºC for 3 h. A new orange complex RhCl(IPr){κ-N,(NC$_5$H$_4$)-2-

CH_2CN}{κ-*N*,NCH_2-2-(C_5H_4N)} (**10**) was isolated in 72 % yield, resulting from the replacement of coe by a 2-pyridylacetonitrile ligand which is coordinated through the nitrogen atom of the nitrile group. No other products were apparent on the NMR spectra.

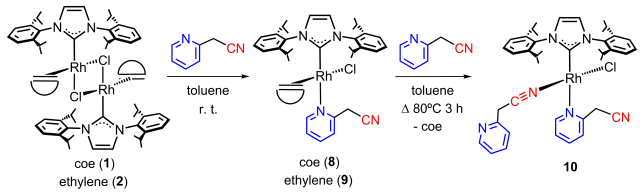

Scheme 3. Preparation of 2-pyridylacetonitrile rhodium complexes.

Complex **8** was characterized by X-ray diffraction analysis. The molecular structure is displayed in figure 1. The mode of coordination of the N-donor ligand was corroborated in the solid state. The metallic center presents a distorted square-planar geometry with the nitrogenated ligand located *trans* to the IPr {C(1)-Rh-N(3) = 167.35(7)°}. The rhodium-carbon separation [Rh–C(1) = 1.9835(18) Å] compares well with previously reported Rh-NHC bond distances.[3c,12] Either the wingtips of the IPr, coe or pyridylacetonitrile ligands adopt an out-of-plane disposition from the square-planar metal environment.

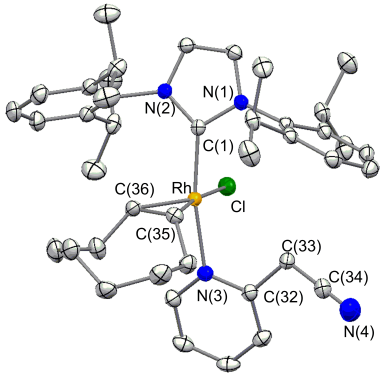

Figure 1. Molecular diagram for **8**. Selected bond lengths (Å) and angles (º): Rh-C(1) = 1.9835(18), Rh-N(3) = 2.1329(16); Rh-C(35) = 2.1383(19), Rh-C(36) = 2.1066(19), C(35)-C(36) = 1.402(3); C(1)-Rh-N(3) = 167.35(7), C(1)-Rh-C(35) = 95.19(7), C(1)-Rh-C(36) = 94.47(8), C(1)-Rh-Cl = 88.27(5).

The ^{1}H and ^{13}C{^{1}H} NMR spectra of **8** and **9** are consistent with the structure shown in figure 1. The presence of a substituent in the 2-position of the pyridine ligand hinders rotation of both IPr[15] and 2-pyridylacetonitrile ligands resulting in an asymmetric molecule. Thus, four and eight signals were observed respectively for the CH and CH_3 isopropyl-IPr substituents. The four inequivalent protons of coordinated ethylene in **9** appeared as doublet of doublets at 2.63, 2.22, 1.91, and 1.37 ppm with homonuclear couplings of 11.3 and 8.2 Hz. Notably, the diastereotopic methylene protons of the dangling nitrile group were observed as doublets at δ 5.79 and 3.76 ppm, (J_{H-H} = 20.0 Hz) for **8** or 4.97 and 3.98 ppm (J_{H-H} = 20.1 Hz) for **9**. In the ^{13}C{^{1}H}-APT NMR spectra, the resonances assigned to carbon atoms directly bonded to rhodium appeared as doublets around 183 ppm (J_{C-Rh} = 54 Hz) for IPr, 60.0 (J_{C-Rh} = 16.6 Hz) and 52.8 ppm (J_{C-Rh} = 14.1 Hz) for coe and 44.8 (J_{C-Rh} = 17.6 Hz) and 37.4 ppm (J_{C-Rh} = 15.8 Hz) for ethylene. The ^{1}H-^{15}N HMBC spectrum of **8** confirmed the coordination of the pyridine motif, δ 270.5 vs 315.2 ppm for the free 2-pyridylacetonitrile.[12i]

The proposed structure for complex **10** was supported by NMR spectra. The ^{1}H spectrum displayed two sets of signals for both methylene groups of either N-donor ligand, one broad signal at 3.32 ppm integrating for two protons and two doublets at 2.75 and 2.67 ppm each integrating for one proton. Similarly to **8** and **9**, the two doublet resonances were ascribed to a κ-N,pyridine coordinated *trans* to IPr, whereas the broad resonance corresponds to a 2-pyridylacetonitrile ligand coordinated through the nitrile moiety in *cis* position to IPr.[16] In fact, a dynamic behaviour with the nitrogenated molecule in solution can be inferred from the ^{1}H-^{15}N HMBC spectrum. The signal corresponding to nitrogen atom of the pyridine appears at δ 315.6 ppm, close to the free ligand value, whereas the nitrile-nitrogen atom resonates at 241.9 ppm, with a deviation of 12 ppm high field shifted indicating coordination to metal centre. In addition, the ^{13}C{^{1}H}-APT NMR spectrum displays just one deshielded doublet at 168.9 ppm with J_{C-Rh} = 50.5 Hz, corresponding to the IPr ligand and two set of carbon atoms for each pyridylacetonitrile ligands. Moreover, an NMR sample of **10** in CD_3CN showed the disappearance of the signals corresponding to the κ-*N*,cyano ligand and not those of the κ-*N*,pyridine group, while resonances corresponding to free 2-pyridylacetonitrile emerged due to an exchange process with the deuterated solvent.

Preparation of phosphine complexes

The observed coordination preference of N-donor ligands to bulky NHC-rhodium-chlorido square-planar complexes may arise from electronic or steric factors. Thus, comparison with other ubiquitous ligands in organometallic catalysis as triphenylphosphine was undertaken. Treatment of RhCl(IPr)(PPh_3)$_2$ (**11**) with pyridine at room temperature for 20 min led to the formation of RhCl(IPr)(PPh_3)(py) (**12**), by phosphine-pyridine exchange,[17] which was isolated as a yellow solid in 83 % yield (Scheme 4). In a similar way to the observed for the dinuclear complexes **1**-**2**, only the phosphine *trans* to IPr was replaced by pyridine, even when neat pyridine was used as solvent.

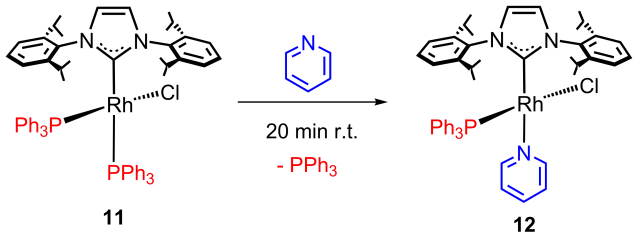

Scheme 4. Pyridine-phosphine exchange reaction leading to RhCl(IPr)(PPh_3)(py) (**12**).

Single crystals of **12** were obtained by slow diffusion of *n*-hexane over a saturated toluene solution of the compound. A

view of the molecular structure is depicted in Figure 2. Similarly to **8**, the metal in **12** presents a distorted square-planar geometry with the pyridine located *trans* to the IPr {C(1)-Rh-N(3) = 172.19(7)°} and a rhodium-carbon separation of 1.9761(19) Å. A significative π–π stacking between the pyridine ligand and a phenyl group was evident from the structural data (centroid-centroid distance 3.656 Å; dihedral angle between planes 20.2º) with potential implications both on structure stability and on fluxional (rotational) behaviour.

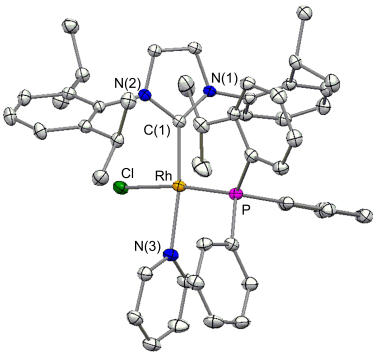

Figure 2. Molecular diagram for **12**. Selected bond lengths (Å) and angles (º): Rh-C(1) = 1.9761(19), Rh-N(3) = 2.1089(17), Rh-P = 2.2124(6); C(1)-Rh-N(3) = 172.19(7), C(1)-Rh-P = 98.22(6), N(3)-Rh-P = 89.29(5), Cl-Rh-P = 172.24(2).

The NMR data for **12** in C_6D_6 are in agreement with the structure observed in the solid state. The $^{31}P\{^1H\}$ NMR spectrum displays a doublet at δ 45.3 ppm with a $J_{P\text{-}Rh}$ = 222.0 Hz, typical for a *trans* chlorido-phosphine complex,[12a] whereas the IPr carbon atom shows in the $^{13}C\{^1H\}$ NMR spectrum a small C-P coupling of 15.6 Hz in accordance with a *cis* carbene-phosphine disposition.

The coordination of the bulky triphenylphosphine ligand *cis* to the hindered IPr in **12** is rather surprising. The high *trans-effect* of the IPr ligand should promote the exchange of the *trans* phosphine in **11**, thus favouring kinetically the isomer observed for **12**. However, this configuration is also thermodynamically favoured as no isomerization was observed on heating a sample of **12** at 60 ºC for 2 h. DFT calculations on the ground state are in accordance with experimental results (Figure 3). Isomer **12at** with the pyridine located *trans* to IPr[18] is 5.4 and 5.8 kcal mol^{-1} more stable than those with PPh_3 (**12bt**) and chlorido[19] (**12ct**) in that position. In this case, in contrast to that observed for 2-pyridylacetonitrile coordination in **10**, both phosphine and pyridine suffer from steric hindrance when located *cis* to the bulky IPr, thus, a rational explanation for the preference of PPh_3 to coordinate *cis* to IPr should be its slightly higher π-acceptor capacity with regard to pyridine.[20]

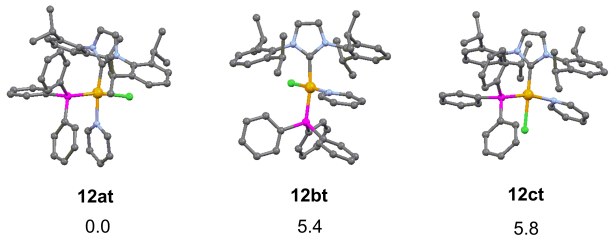

Figure 3. DFT-computed energies for the possible stereoisomers of **12** (ΔE, kcal mol^{-1}).

Acetonitrile behaves in a different way than pyridine does. Treatment of **11** with acetonitrile at room temperature resulted in the isolation of the starting material, similarly to that observed for **1** and **2**. However, a sample of **11** dissolved in CD_3CN led to the *in-situ* formation of two isomers of the complex $RhCl(IPr)(PPh_3)(CD_3CN)$ (**13**) in a 70:30 ratio (Scheme 5).[21] The $^{31}P\{^1H\}$ NMR spectrum displays, in addition to a signal corresponding to free PPh_3, two new doublets at 41.9 and 22.3 ppm with $J_{P\text{-}Rh}$ of 206.7 and 89.4 Hz, respectively. In accordance with that observed for phosphine-pyridine complex **12**, the derivative with the highest rhodium-phosphine scalar coupling was ascribed to the isomer having a *cis* IPr-phosphine configuration (**13a**), whereas the minor isomer presented *trans* IPr-phosphine disposition (**13b**). Complex **13a** seems to be kinetically favoured over **13b**. A CD_3CN solution of **12** showed the exclusive formation of **13a** resulting from the pyridine/acetonitrile exchange. Heating the sample at 60 ºC for 48 h gave rise to the formation of a new cationic bis-acetonitrile complex $[Rh(IPr)(PPh_3)(CH_3CN)_2]Cl$ (**14**), with a phosphine-carbene *trans* disposition (Figure 4). The same complex was obtained on heating a mixture of **13a** and **13b** arising from **11**. The stabilization gained from a mutually *trans* disposition of acetonitrile ligands in **14** would likely account for the formation of only one isomer with phosphine-carbene *trans* configuration.

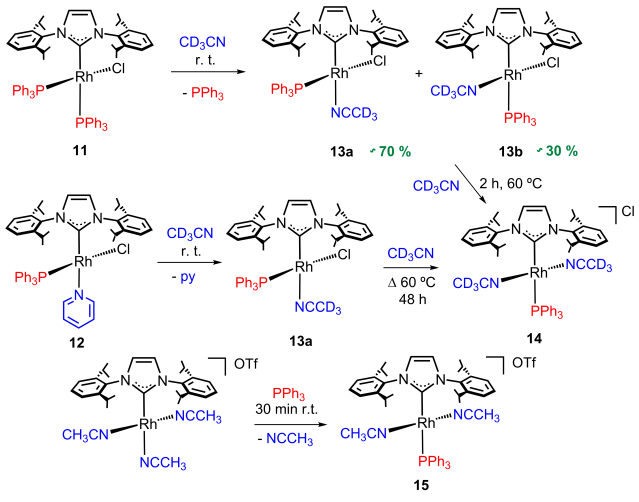

Scheme 5. Formation of rhodium-phosphine-acetonitrile complexes.

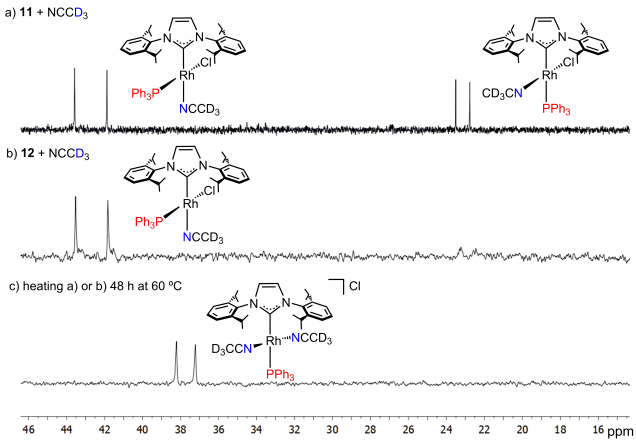

Figure 4. $^{31}P\{^{1}H\}$ NMR spectra of **13** and **14**.

The triflate (OTf) salt of **14**, [Rh(IPr)(PPh_3)(CH_3CN)$_2$]OTf (**15**), has been independently prepared by treatment of the cationic derivative [Rh(IPr)(CH_3CN)$_3$]OTf[12h] with PPh_3. The more noticeable features of the NMR spectra of **15** are the doublet at δ 37.1 ppm with a $J_{P\text{-}Rh}$ of 120.7 Hz in the $^{31}P\{^{1}H\}$ NMR spectrum, and the resonance at δ 185.3 ppm (dd, $J_{C\text{-}P}$ of 114.6 Hz, and $J_{C\text{-}Rh}$ of 46.5 Hz) in the $^{13}C\{^{1}H\}$ for the carbene carbon atom indicating a *trans* IPr-phosphine configuration. DFT calculations on the ground state of **13** show that, in contrast to that observed for pyridine-phosphine isomers of **12**, both isomers of **13** present very similar computed energies (Figure 5).

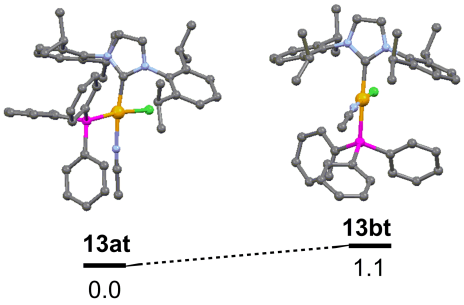

Figure 5. DFT-computed energies for possible stereoisomers of **13** (ΔE, kcal mol^{-1}).

In contrast to the behaviour observed for complexes containing PPh_3 ligands, treatment of Rh^{I}-NHC dimer **1** with a bulkier and more electron-rich phosphine such as tricyclohexylphosphine (PCy_3) in N-donor solvents led to different results (Scheme 6). The phosphine did not incorporate into the metallic complex in pyridine solutions at 60 ºC for one night and pure Rh-NHC-pyridine complex **3a** was isolated. However, a new NHC-phosphine complex RhCl(IPr)(PCy_3)(CH_3CN) (**16**) was obtained from acetonitrile solutions after 30 min at 60 ºC. The $^{31}P\{^{1}H\}$ NMR spectrum in CD_3CN of **16** displays a doublet at δ 34.6 ppm with $J_{P\text{-}Rh}$ of 118.8 Hz, indicating a *trans* NHC-phosphine disposition. Moreover, the carbene carbon atom resonates in the in the $^{13}C\{^{1}H\}$-APT NMR spectrum as a doublet of doublets at δ 188.8 ppm with typical couplings $J_{C\text{-}Rh}$ of 44.3 Hz and $J_{C\text{-}P}$ of 106.9 Hz, corroborating the proposed configuration. These results can be rationalized assuming the high steric encumbrance of PCy_3 and the affinity of pyridine for *trans*-to-IPr coordination.

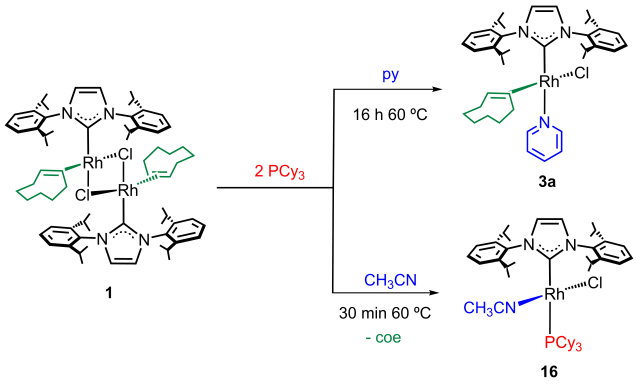

Scheme 6. Reactivity of **1** with PCy_3 in different nitrogenated solvents.

Coordination of small molecules

In order to broaden the study of the effect of IPr over coordination of the ancillary ligands in square-planar Rh^{I} complexes, the reactivity with small molecules such as CO and dioxygen was also investigated. Treatment of **1** or **3a** with CO in pyridine as solvent at room temperature led to the formation of RhCl(IPr)(CO)(py) (**17**) (Scheme 7). In contrast, bubbling carbon monoxide through a solution of **1** in acetonitrile led to the isolation of the bis-carbonyl complex RhCl(IPr)(CO)$_2$.[12b] The coordination of pyridine *trans* to IPr of **17** was substantiated by the high $J_{C\text{-}Rh}$ coupling constant (82.0 Hz) displayed for the CO carbon atom in the $^{13}C\{^{1}H\}$ NMR spectrum, which is typical for a mutually *trans* chlorido-CO disposition.[22] ^{1}H VT-NMR spectra of **17** in CD_2Cl_2, showed a dynamic behaviour as result of carbene rotation around the Rh-IPr bond (Figure 6).[15] The activation parameters obtained from the corresponding Eyring analysis were $\Delta H^{\ddagger}$ = 10.6 ± 0.3 kcal·mol^{-1} and $\Delta S^{\ddagger}$ = 0.2 ± 0.6 cal·K^{-1} mol^{-1} which lay in the range of those previously reported for Rh-IPr complexes.[6,12h,15]

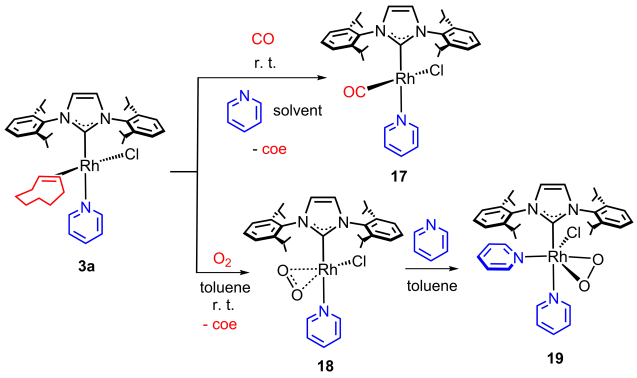

Scheme 7. Reactivity of **3a** with small molecules.

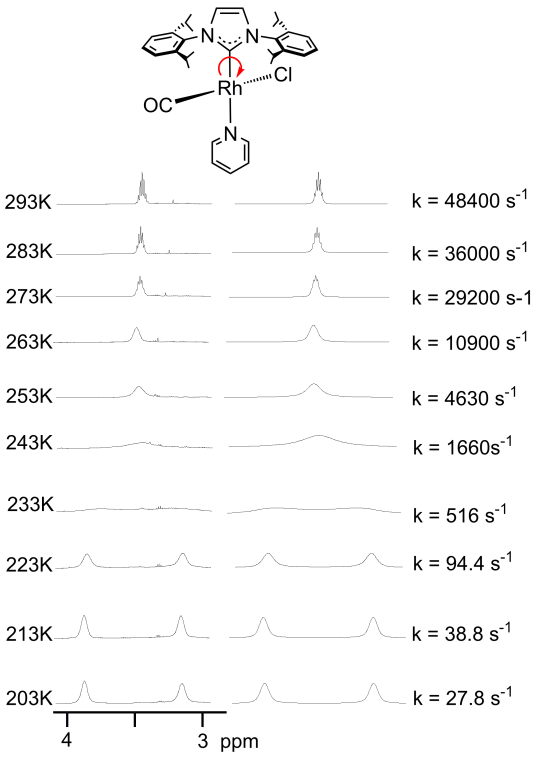

Figure 6. Variable temperature NMR spectra of **17** in CD_2Cl_2 showing the coalescence of the CH-isopropyl (IPr): experimental (left) and calculated (right).

Complex **3a** reacts very fast with molecular oxygen. Bubbling air through a toluene solution of **3a** for 15 min at room temperature resulted in the formation of complex RhCl(IPr)(O_2)(py) (**18**), that was isolated as a green solid in 70 % yield. Prolonged reaction times under air gave rise to unidentified products, as previously described by the Crudden´s group.[12f] We were not able to isolate any clean complex from the similar treatment of **1** in acetonitrile solutions. Addition of pyridine to **18** led to the formation of the bis-pyridine adduct RhCl(IPr)(O_2)(py)$_2$ (**19**) which was isolated as a yellow solid in 75% yield. The coordination of dioxygen to transition metal complexes very often results in the formation of monodentated dioxygen adducts {$^1O_2$} or peroxo {O_2^{2-}} complexes.[23] In this particular case, complex **18** is better described as a tetracoordinated $Rh^I\{^1O_2\}$[24] species whereas **19** points to a $Rh^{III}\{O_2^{2-}\}$[25] hexacoordinated compound. Suitable single crystals for X-ray determination were obtained by slow diffusion of *n*-hexane into saturated toluene solutions of **18** and **19**. A diagram of the molecular structures is shown in figure 7.

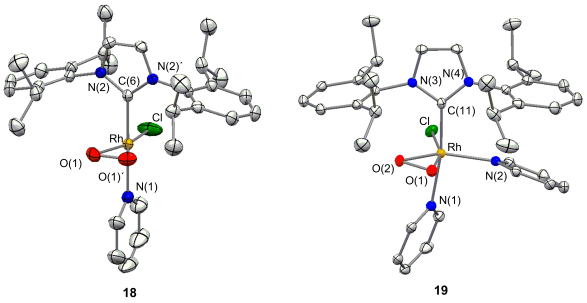

Figure 7. Molecular diagram for **18** and **19**. Selected bond lengths (Å) and angles (º), **18**: Rh-C(6) = 1.984(3), Rh-O(1) = 1.959(5), Rh-N(1) = 2.146(3), O(1)-O(1)´ = 1.424(11), Rh-Cl = 2.287(2); C(6)-Rh-N(1) = 178.33(12), O(1)-Rh-O´(1) = 42.6(3), O(1)-Rh-N(1) = 88.73(17); **19**: Rh-C(11) = 2.0081(17), Rh-O(1) = 1.9884(12), Rh-O(2) = 1.9819(13), Rh-N(1) = 2.1541(15), Rh-N(2) = 2.1462(15), O(1)-O(2) = 1.4399(17), Rh-Cl = 2.4057(4); C(11)-Rh-N(1) = 170.67(6), C(11)-Rh-N(2) = 101.44(6), O(1)-Rh-O(2) = 42.53(5), O(1)-Rh-N(2) = 109.33(5), Cl-Rh-O(2) = 118.83(4), N(1)-Rh-N(2) = 87.80(6), C(11)-Rh-Cl = 89.37(5).

Complex **18** shows a square-planar structure with a carbene-pyridine *trans* disposition {C(6)-Rh-N(1) = 178.33(12)°}, typical of Rh^I species, whereas compound **19** is better described as a distorted octahedron with one pyridine ligand *trans* to IPr {C(11)-Rh-N(1) = 170.67(6)°} and the other nitrogenated ligand *cis* disposed {C(11)-Rh-N(2) = 101.44(6)°} more characteristic of Rh^{III} complexes. The O−O distance in **19** {1.4399(17)} lies within the range described for Rh-peroxo complexes (1.43-1.50 Å). The dioxygen separation in **18** {1.424(11) Å} is only slightly shorter than that in **19**, with its accuracy affected by the positional disorder of the ligand (see experimental). However, the O-O stretching mode in the IR spectra was observed at 965 cm^{-1} for **18** and 879 cm^{-1} for **19**, which reflects the different character of the dioxygen ligand in both complexes. The formation of the oxidized complex **19** is likely favoured by the ability of **18** to easily accommodate a new ligand, a pyridine in this case, changing the coordination mode of the dioxygen molecule.

The NMR spectra of **18** are in agreement with a IPr-pyridine *trans* coordination in a C_s-symmetric compound. In contrast, the NMR of **19** in CD_2Cl_2 showed no equivalent pyridine ligands and also evidenced the presence of a symmetry plane that makes equivalent two isopropyl groups which points to the ionization of the chlorido ligand in solution to give the [Rh(IPr)(O_2)(py)$_2$]Cl species. Similarly to **17**, complexes **18** and **19** showed a dynamic behaviour as evidenced in a ^{1}H VT-NMR study due to IPr rotation. The activation parameters obtained from the corresponding Eyring analysis were $\Delta H^{\ddagger}$ = 9.9 ± 0.6 kcal·mol^{-1} and $\Delta S^{\ddagger}$ = -4.2 ± 1.7 cal·K^{-1} mol^{-1} for **18** and $\Delta H^{\ddagger}$ = 13.0 ± 0.7. kcal·mol^{-1} and $\Delta S^{\ddagger}$ = 2.8 ± 1.5 cal·K^{-1} mol^{-1} for **19**. The rotational barrier for **18** is the lowest ever calculated for similar Rh^I-IPr complexes (Table 1). It is generally assumed that the steric hindrance of the auxiliary ligands on the Rh-IPr motif play a fundamental role in the activation barriers for the rotation.[15] For example, the phosphine complex RhCl(IPr)(η^2-CH_2=CH_2)(PPh_3)[15] show the higher value (entry 2, table 1). In addition, η^2-coe complexes have slightly higher values than η^2-ethylene ones (entries 4 *vs* 5 and 6 *vs* 7, table 1). Nevertheless, a

bulky environment is not the sole factor that contributes to the rotational barrier. It has been proposed that the lone pair of electrons of a π-donor ligand such as chlorido may interact with the empty p-orbital of the NHC,[26] thus affecting the rotation. In the present case, the chlorido-IPr complex **3a** exhibits a higher rotational barrier (15.1 ± 0.7 kcal·mol^{-1}, entry 4, table 1) than the acac-IPr complex (12.7 ± 0.4 kcal·mol^{-1}, entry 6, table 1) or a cationic free-chlorido derivative (12.7 ± 0.3 kcal·mol¯1, entry 8, table 1).

Table 1. Comparison of rotational barriers for various Rh^{I}-IPr complexes.[a]

Entry	Complex	$\Delta H^{\neq}$ (kcal·mol^{-1})
1	RhCl(=CHPh)(IPr)PPh_3[15h]	13.4 ± 0.8
2	RhCl(η^2-CH_2=CH_2)(IPr)PPh_3[15h]	16.6 ± 0.7
3	[Rh(μ-Cl)(IPr)(η^2-CH_2=CH_2)]$_2$ (**2**)[6]	11.8 ± 0.4
4	RhCl(IPr)(py)(η^2-coe) (**3a**)[6]	15.1 ± 0.7
5	RhCl(IPr)(py)(η^2-ethylene) (**3b**)[6]	14.1 ± 0.6
6	Rh(acac)(IPr)(η^2-coe)[12h]	12.7 ± 0.4
7	Rh(acac)(IPr)(η^2-ethylene)[12h]	10.4 ± 0.3
8	[Rh(IPr)(η^2-coe)($NCCH_3$)$_2$]OTf[12h]	12.7 ± 0.3
9	RhCl(IPr)(CO)(py) (**17**)	10.6 ± 0.3
10	RhCl(IPr)(O_2)(py) (**18**)	9.9 ± 0.6
11	RhCl(IPr)(O_2)(py)$_2$ (**19**)	13.0 ± 0.7

[a] acac = acetylacetonate, OTf = CF_3SO_3

Charge Decomposition Analysis (CDA) on square-planar Rh-IPr-Chlorido complexes

The relative stability observed in phosphine-pyridine derivative **12** in favour of a more hindered *cis* phosphine-IPr configuration indicates a notable influence of electronic factors over the whole stability of the square-planar complexes. Thus, we have performed a Charge Decomposition Analysis (CDA)[27] between the metallic fragment and the π-acceptor ligand in order to better explain the observed results. This method provides a deeper insight into the nature of the acceptor-donor interactions and it has been extensively used to analyse the metal-ligand bonds in organometallic complexes[28] according to the model of Dewar-Chatt-Duncanson.[29] In particular the method allows a measurement of the electron donation of the ligand to the metal fragment (σ-donation) and the back-donation from the metal centre to the ligand moiety (π-backbonding) to be obtained. In our case the analysis was carried out by measuring the interaction of two distinct metal fragments [RhCl(IPr)(py)]− derived from **12a** (fragment A) and **12b** (fragment B) with a set of different ligands (Scheme 8, Table 2).

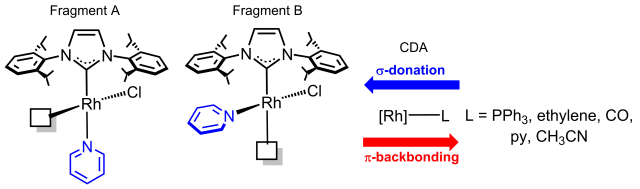

Scheme 8. CDA study of the bond between metallic fragments A and B with different ligands.

Table 2. CDA calculations for fragments A and B.

Entry	Ligand	Fragment A			Fragment B		
		L→Rh[a]	Rh→L	BE[b]	L→Rh	Rh→L	BE
1	ethylene	0.591	0.347	61.4	0.565	0.246	44.0
2	CO	0.518	0.417	67.9	0.553	0.334	50.7
3	PPh_3	0.396	0.377	65.0	0.322	0.176	49.9
4	pyridine	0.235	0.124	40.9	0.251	0.063	31.9
5	CH_3CN	0.282	0.173	36.2	0.298	0.083	25.6

[a] Total electrons, sum of contributions from all orbitals. [b] bond energy in kcal mol^{-1}

Table 2 summarises the results obtained with respect to L → [Rh] σ-donation, [Rh] → L π-backbonding and the bonding energy between fragments A or B and the ligand. In all cases bonding energy was higher for fragment A. Nevertheless, σ-donation values are always comparable for fragments A and B, thus π-backbonding values should account for the measured differences in bonding energies. Such evidence suggests that coordination in *cis* position to the NHC ligand allows for a more efficient π-backbonding and consequently, it is the favoured coordination site for π-acceptor ligands such as CO or PPh_3 in **12a**. As expected, pyridine and acetonitrile show both lower π-acceptor ability but pyridine displays slightly higher bond energy than acetonitrile, in agreement with the formation of **8-9**.

In the analysed case CDA-analysis suggest how the M-L bond is the result of a complex series of interactions. In the case of complex **12a**, CDA analysis revealed two prevalent interactions (Scheme 9). HOMO -7 represents the L → [Rh] σ-donation and contributes to 10.2 kcal mol^{-1} of the total binding energy of 65.0 kcal mol^{-1}. It involves a donation of 0.092 electron of 0.396 (23% of the total σ-donation) from PPh_3 to the metallic fragment. The second most relevant interaction refers to HOMO -1 which is the one providing for a 0.126 electrons of 0.377 (34%) of π-backbonding from Rh to PPh_3, contributing to the total binding energy with 8.2 Kcal mol^{-1}.

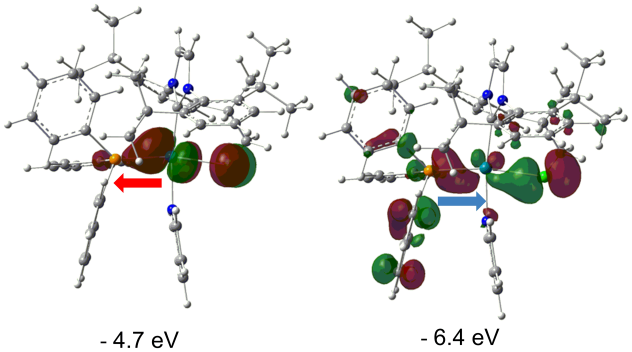

Figure 8. Selected molecular orbitals with corresponding energies for complex **12a**.

Concluding Remarks

The electronic and steric factors that control the coordination chemistry of N-donor ligands in a Rh^{I}-NHC-chlorido square-planar framework have been disclosed. Both experimental and theoretical results indicate that pyridine shows a clear tendency to coordinate *trans* to IPr whereas π-acceptor ligands bind preferentially *cis* to IPr and *trans* to chlorido (olefin, CO or PPh_3), unless steric bulk hinders the coordination of the ligand (PCy_3). In contrast, acetonitrile binds weaker than pyridine does, but it is able to form *cis*-to IPr complexes. In this system ethylene forms stronger coordination bonds than coe. CDA analysis shows that σ-donation values are similar for *cis*- or *trans*-IPr coordination, whereas π-backbonding is significantly increased in *cis* position. Molecular dioxygen displaces the labile cyclooctene ligand in these square-planar complexes to give a dioxygen adduct or a peroxo complex in function of the number of pyridine ligands coordinated at the rhodium centre. The influence of ancillary ligands on the Rh-IPr rotational barrier is mainly steric in origin. However, the presence of a π-donor ligand such as chlorido, also slows down the dynamic process. The basic knowledge on coordination chemistry reported in this work is being applied in our group for the design of more efficient catalysts for C-C and C-X couplings based on the Rh-NHC framework.

Acknowledgement

Financial support from the spanish Ministerio de Economía y Competitividad (MINECO/FEDER) (CTQ2013-42532-P and CONSOLIDER INGENIO CSD2009-0050 projects), the Diputación General de Aragón (DGA/FSE-E07), the ARAID Foundation under the program "*Jóvenes Investigadores*", and the Campus Iberus, are gratefully acknowledged. ADG thanks the "subprograma de Formación Postdoctoral" from the Spanish MINECO.

Experimental part

All reactions were carried out with rigorous exclusion of air using Schlenck-tube techniques. Organic solvents were dried by standard procedures and distilled under argon prior to use or obtained oxygen- and water- free from a Solvent Purification System (Innovative Technologies). The starting materials **1**,[12a] **2**,[6] **3a**,[6] **11**,[12a] and **15**[12h] were prepared as previously described in the literature. Chemical shifts (expressed in parts per million) are referenced to residual solvent peaks (^{1}H, ^{13}C) or external H_3PO_4 (^{31}P), $CFCl_3$ (^{19}F) or liquid NH_3 (^{15}N). Coupling constants, *J* and *N*, are given in hertz. Spectral assignments were achieved by combination of ^{1}H-^{1}H COSY, ^{13}C-APT, and ^{1}H-^{13}C HSQC/HMBC experiments. C, H, and N analyses were carried out in a Perkin-Elmer 2400 CHNS/O analyzer. Infrared spectra were recorded on a Perkin-Elmer Spectrum 100 spectrometer, using a Universal ATR Sampling Accesory (neat samples).

Reactivity of 1 or 2 with acetonitrile. A solution of **1** (100 mg, 0.079 mmol) or **2** (100 mg, 0.091 mmol) in a mixture of toluene (2 mL) and acetonitrile (2 mL) was stirred at room temperature for 3 h. Then, the solution was concentrated to ca. 1 mL and *n*-hexane added to induce the precipitation of a orange solid, which was washed with *n*-hexane (3 x 3 mL) and dried in vacuo, corresponding to the starting complex.

***In-situ* formation of RhCl(IPr)(η^2-CH_2=CH_2)(CH_3CN) (4)**. A solution of **2** (15 mg, 0.014 mmol) in toluene-d_8 (0.5 mL, NMR tube) was treated with 100 µL of acetonitrile. ^{1}H NMR (300 MHz, toluene-d_8, 253 K): δ 7.4-6.9 (6H, H_{Ph}), 6.66 (s, 2H, =CHN), 3.75 and 2.77 (both sept, J_{H-H} = 6.5, 4H, C<u>H</u>Me_{IPr}), 2.47 and 2.33 (both d, J_{H-H} = 12.3, 4H, CH_2=CH_2), 2.15 (s, 3H, CH_3CN), 1.65, 1.43, 1.06, and 1.02 (all d, J_{H-H} = 6.5, 24H, CH<u>Me</u>$_{IPr}$). $^{13}C\{^{1}H\}$-APT NMR (75.1 MHz, toluene-d_8, 253 K): δ 181.4 (d, J_{C-Rh} = 56.7, Rh-C_{IPr}), 147.7 and 145.5 (both s, C_{q-IPr}), 137.2 (s, C_qN), 129.4, 124.3, and 123.7 (all s, CH_{Ph-IPr}), 124.3 (s, =CHN), 118.5 (s, CH_3<u>C</u>N), 41.8 (d, J_{C-Rh} = 15.4, CH_2=CH_2), 28.6 and 28.5 (both s, <u>C</u>HMe$_{IPr}$), 25.9, 25.7, 23.4, and 22.9 (all s, CH<u>Me</u>$_{IPr}$), 0.3 (br, <u>C</u>H_3CN).

Preparation of [Rh(IPr)(CH_3CN)$_3$]Cl (5). An acetonitrile solution (10 mL) of **1** (100 mg, 0.079 mmol) was heated at 80ºC for 5 h. After removing the solvent in vacuo, addition of *n*-hexane at caused the precipitation of a pale brown solid which was washed with *n*-hexane (3 x 3 mL) and dried in vacuo. ^{1}H NMR and $^{13}C\{^{1}H\}$ spectra match with that of [Rh(IPr)(CH_3CN)$_3$]OTf described previously.[12h]

Preparation of RhCl(IPr)(η^2-coe)\{η^1-N(C_5H_4)-2-CH_2CN\} (8). An orange solution of **1** (300 mg, 0.236 mmol) in toluene (10 mL) was treated with 2-pyridylacetonitrile (28 µL, 0.25 mmol) and it was stirred at room temperature for 1 h. Then, the solvent was removed in vacuo and addition of *n*-hexane caused the precipitation of a yellow solid which was washed with *n*-hexane (3 x 3 mL) and dried in vacuo. Yield: 278 mg (78%). Anal. Calcd. for $C_{42}H_{56}N_4ClRh$: C, 66.79; H, 7.47; N, 7.42. Found: C, 66.93; H, 7.52; N, 7.48. ^{1}H NMR (500 MHz, toluene-d_8, 253 K): δ 8.19 (d, J_{H-H} = 5.1, 1H, H_{6-py}), 7.3-7.0 (m, 6H, H_{Ph-IPr}), 6.46 (dd, J_{H-H} = 9.0, 7.7, 1H, H_{4-py}), 6.86 (d, J_{H-H} = 7.7, 1H, H_{3-py}), 6.61 and 6.51 (both d, J_{H-H} = 1.7, 2H, =CHN), 6.08 (dd, J_{H-H} = 9.0, 5.1, 1H, H_{5-py}), 5.79 and 3.76 (both d, J_{H-H} = 20.0, 2H, CH_{2-py}), 4.66, 3.79, 2.72, and 2.02 (all sept, J_{H-H} = 6.5, 4H, C<u>H</u>Me_{IPr}), 3.0 (m, 2H, $=CH_{coe}$), 1.96, 1.53, 1.43, 1.21, 1.18, 1.06, 1.00, and 0.84 (all d, J_{H-H} = 6.5, 24H, CH<u>Me</u>$_{IPr}$), 1.6-0.3 (br, 12H, CH_{2-coe}). $^{13}C\{^{1}H\}$-APT NMR (125.6 MHz, toluene-d_8, 253 K): δ 183.3 (d, J_{C-Rh} = 54.3, Rh-C_{IPr}), 154.5 (s, C_{2-py}), 152.4 (s, C_{6-py}), 149.0, 148.3, 146.5, and 146.0 (all s, C_{q-IPr}), 137.2 and 136.8 (both s, C_qN),

135.8 (s, $C_{4\text{-py}}$), 130.2, 129.8, 124.6, 123.1, 122.9, and 122.6 (all s, $CH_{Ph\text{-IPr}}$), 124.4 and 123.9 (s, =CHN), 122.8 (s, $C_{3\text{-py}}$), 121.4 (s, $C_{5\text{-py}}$), 117.0 (CN_{py}), 60.0 (d, $J_{C\text{-Rh}}$ = 16.6, $=CH_{coe}$), 52.8 (d, $J_{C\text{-Rh}}$ = 14.1, $=CH_{coe}$), 30.7, 30.4, 29.3, 29.1, 26.7, and 26.5 (all s, $CH_{2\text{-coe}}$), 29.7, 29.4, 28.6, and 28.5 (all s, $\underline{C}HMe_{IPr}$), 27.7 (s, $CH_{2\text{-py}}$), 27.6, 26.8, 26.3, 26.2, 24.9, 23.1, 23.0, and 21.6 (all s, $CH\underline{Me}_{IPr}$). ^{15}N-^{1}H HMBC (40 MHz, toluene-d_8, 298 K): δ 270.5 (N_{py}), 190.0 and 189.8 (N_{IPr}).

Preparation of RhCl(IPr)(η^2-CH_2=CH_2){η^1-N(C_5H_4)-2-CH_2CN} (9). The complex was prepared as described for **8** starting from **2** (300 mg, 0.270 mmol) and 2-pyridylacetonitrile (32 µL, 0.29 mmol). Yield: 325 mg (89%). Anal. Calcd. for $C_{36}H_{46}N_4ClRh$: C, 64.23; H, 6.89; N, 8.32. Found: C, 64.56; H, 6.99; N, 8.38. ^{1}H NMR (500 MHz, toluene-d_8, 253 K): δ 7.86 (d, $J_{H\text{-H}}$ = 5.2, 1H, $H_{6\text{-py}}$), 7.3-7.0 (m, 6H, $H_{Ph\text{-IPr}}$), 6.38 (dd, $J_{H\text{-H}}$ = 9.2, 7.5, 1H, $H_{4\text{-py}}$), 6.75 (d, $J_{H\text{-H}}$ = 7.5, 1H, $H_{3\text{-py}}$), 6.59 and 6.44 (both d, $J_{H\text{-H}}$ = 1.5, 2H, =CHN), 5.95 (dd, $J_{H\text{-H}}$ = 9.2, 5.2, 1H, $H_{5\text{-py}}$), 4.97 and 3.98 (both d, $J_{H\text{-H}}$ = 20.1, 2H, $CH_{2\text{-py}}$), 4.24, 3.73, 2.92, and 2.35 (all sept, $J_{H\text{-H}}$ = 6.5, 4H, $C\underline{H}Me_{IPr}$), 2.63, 2.22, 1.91, and 1.37 (all dd, $J_{H\text{-H}}$ = 11.3, 8.2, 4H, CH_2=CH_2), 1.88, 1.63, 1.46, 1.30, 1.16, 1.06, 1.05, and 0.93 (all d, $J_{H\text{-H}}$ = 6.5, 24H, $CH\underline{Me}_{IPr}$). $^{13}C\{^{1}H\}$-APT NMR (125.6 MHz, toluene-d_8, 253 K): δ 182.8 (d, $J_{C\text{-Rh}}$ = 54.2, Rh-C_{IPr}), 153.7 ($C_{2\text{-py}}$), 149.7 (s, $C_{6\text{-py}}$), 149.1, 148.3, 146.4, and 145.7 (all s, $C_{q\text{-IPr}}$), 137.1 and 137.0 (both s, C_qN), 135.9 (s, $C_{4\text{-py}}$), 129.9, 129.1, 124.9, 124.4, 123.2, and 122.9 (all s, $CH_{Ph\text{-IPr}}$), 124.4 and 123.9 (both s, =CHN), 122.7 (s, $C_{3\text{-py}}$), 122.5 (s, $C_{5\text{-py}}$), 116.6 (s, CN_{py}), 44.8 (d, $J_{C\text{-Rh}}$ = 17.6, CH_2=CH_2), 37.4 (d, $J_{C\text{-Rh}}$ = 15.8, CH_2=CH_2), 27.0 (s, $CH_{2\text{-py}}$), 29.7, 29.4, 28.7, and 28.7 (all s, $\underline{C}HMe_{IPr}$), 27.3, 26.8, 26.3, 25.9, 24.5, 23.0, 22.9, and 22.0 (all s, $CH\underline{Me}_{IPr}$).

Preparation of RhCl(IPr){(η^1-N(C_5H_4)-2-CH_2CN}{(η^1-$NCCH_2$-2-(C_5H_4)N} (10). A solution of **8** (150 mg, 0.198 mmol) in toluene (10 mL) was treated with 2-pyridylacetonitrile (25 µL, 0.22 mmol) and was heated at 80ºC for 3 h. Then, the solution was concentrated to ca. 1 mL and *n*-hexane added to induce the precipitation of a yellow solid, which was washed with *n*-hexane (3 x 3 mL) and dried in vacuo. Yield: 109 mg (72%). ^{1}H NMR (500 MHz, C_6D_6, 298 K): δ 8.34 (d, $J_{H\text{-H}}$ = 4.4, 1H, $H_{6\text{-pyb}}$), 7.59 (br, 1H, $H_{6\text{-pya}}$), 7.3-7.0 (m, 6H, $H_{Ph\text{-IPr}}$), 7.31 (br, 1H, $H_{3\text{-pyb}}$), 7.01 (vt, $J_{H\text{-H}}$ = 6.5, 1H, $H_{4\text{-pyb}}$), 6.73 (s, 2H, =CHN), 6.60 (m, 1H, $H_{5\text{-pyb}}$), 6.57 (vt, $J_{H\text{-H}}$ = 7.7, 1H, $H_{4\text{-pya}}$), 6.20 (br, 1H, $H_{5\text{-pya}}$), 6.01 (d, $J_{H\text{-H}}$ = 7.7, 1H, $H_{3\text{-pya}}$), 3.84 and 3.77 (both sept, $J_{H\text{-H}}$ = 6.6, 4H, $C\underline{H}Me_{IPr}$), 3.32 (br, 2H, $CH_{2\text{-pyb}}$), 2.75 and 2.67 (both d, $J_{H\text{-H}}$ = 10.7, 2H, $CH_{2\text{-pya}}$), 1.84 and 1.25 (both d, $J_{H\text{-H}}$ = 6.6, 24H, $CH\underline{Me}_{IPr}$). $^{13}C\{^{1}H\}$-APT NMR (125.6 MHz, C_6D_6, 298 K):δ 173.0 (s, $C_{2\text{-pya}}$), 168.9 (d, $J_{C\text{-Rh}}$ = 50.5, Rh-C_{IPr}), 150.7 (s, $C_{2\text{-pyb}}$), 149.5 (s, $C_{6\text{-pyb}}$), 147.7 (br, $C_{q\text{-IPr}}$), 145.2 (s, $C_{6\text{-pya}}$), 136.8 (s, $C_{4\text{-pyb}}$), 136.7 (s, C_qN), 134.1 (s, $C_{4\text{-pya}}$), 130.5 (s, $C_{p\text{-Ph}}$), 124.3 (s, =CHN), 124.0 and 123.9 (both s, $C_{m\text{-Ph}}$), 122.4 (s, $C_{5\text{-pyb}}$), 122.2 (s, $C_{3\text{-pyb}}$), 121.2 (s, $C_{5\text{-pya}}$), 119.7 (s, $C_{3\text{-pya}}$), 117.9 (CN_{pyb}), 116.3 (CN_{pya}), 28.7 and 28.5 (both s, $\underline{C}HMe_{IPr}$), 26.5 (s, $CH_{2\text{-pya}}$), 26.4, 26.3, 23.7 and 23.6 (all s, $CH\underline{Me}_{IPr}$), 22.8 (s, $CH_{2\text{-pyb}}$). ^{15}N-^{1}H HMBC (40 MHz, toluene-d_8, 298 K): δ 315.6 (N_{py}), 241.9 (N_{CN}), 193.4 and 192.0 (N_{IPr}).

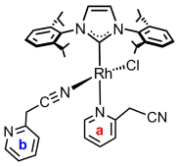

Preparation of RhCl(IPr)(PPh_3)(py) (12). A solution of **11** (355 mg, 0.338 mmol) in pyridine (5 mL) was stirred for 20 min at room temperature. Then, the solution was concentrated to ca. 1 mL and diethyl ether added to induce the precipitation of a yellow solid, which was washed with diethyl ether (3 x 3 mL) and dried in vacuo. Yield: 237 mg (83%). Anal. Calcd. for $C_{50}H_{56}N_3ClPRh$: C, 69.16; H, 6.50; N, 4.84. Found: C, 68.92; H, 6.67; N, 5.07. ^{1}H NMR (300 MHz, C_6D_6, 298 K): δ 8.28 (d, $J_{H\text{-H}}$ = 4.2, 2H, $H_{2\text{-py}}$), 7.5-6.7 (23H, H_{Ph}, =CHN), 6.41 (t, $J_{H\text{-H}}$ = 7.2, 1H, $H_{4\text{-py}}$), 5.93 (dd, $J_{H\text{-H}}$ = 7.2, 4.2, 2H, $H_{3\text{-py}}$), 4.11 and 3.97 (both sept, $J_{H\text{-H}}$ = 6.4, 4H, $C\underline{H}Me_{IPr}$), 2.04, 1.31, 1.12, and 0.82 (all d, $J_{H\text{-H}}$ = 6.4, 24H, $CH\underline{Me}_{IPr}$). $^{13}C\{^{1}H\}$-APT NMR (75.4 MHz, C_6D_6, 298 K): δ 190.8 (dd, $J_{C\text{-Rh}}$ = 53.0, $J_{C\text{-P}}$ = 15.6, Rh-C_{IPr}), 153.4 (s, $C_{2\text{-py}}$), 149.5 and 144.4 (both s, $C_{q\text{-IPr}}$), 138.7 (s, C_qN), 138.1 (d, $J_{C\text{-P}}$ = 35.1, C_qP), 134.2 (d, $J_{C\text{-P}}$ = 12.0, $CH_{o\text{-PPh}}$), 132.7 (s, $C_{4\text{-py}}$), 129.3, 128.5, 127.1, 124.3, and 123.1 (all s, CH_{Ph}), 124.0 (s, =CHN), 121.9 (s, $C_{3\text{-py}}$), 29.3 and 28.3 (both s, $\underline{C}HMe_{IPr}$), 26.7, 26.6, 24.2, and 22.4 (all s, $CH\underline{Me}_{IPr}$). $^{31}P\{^{1}H\}$ NMR (121.5 MHz, C_6D_6, 298 K): δ 45.3 (d, $J_{P\text{-Rh}}$ = 222.0).

***In-situ* formation of RhCl(IPr)(PPh_3)(CD_3CN) (13).** Complex **11** (20 mg, 0.019 mmol) was disolved in CD_3CN (0.5 mL, NMR tube). A mixture 70/30 **13a**/**13b** was observed. $^{31}P\{^{1}H\}$ NMR (161.8 MHz, CD_3CN, 298 K): δ 41.9 (d, $J_{P\text{-Rh}}$ = 206.7, **13a**), 22.3 (d, $J_{P\text{-Rh}}$ = 89.4, **13b**).

Preparation of [Rh(IPr)(PPh_3)(CH_3CN)$_2$]OTf (15). An acetonitrile solution (5 mL) of [Rh(IPr)(CH_3CN)$_3$]OTf (96 mg, 0.11 mmol) was treated with PPh_3 (29 mg, 0.11 mmol). After stirring for 30 min at room temperature, the solution was evaporated to dryness. Addition of *n*-hexane caused the precipitation of a white solid which was washed (3 x 3 mL) and dried in vacuo. Yield: 81mg (74%). Anal.Calcd. for $C_{50}H_{57}N_4SF_3O_3PRh$: C, 60.97; H, 5.83; N, 5.69. S, 3.26. Found: C, 60.73; H, 6.29; N, 5.78; S, 3.17. ^{1}H NMR (400 MHz, CD_3CN, 298 K): δ 7.8-6.9 (m, 19H, H_{Ph}, =CHN), 2.85 (sept, $J_{H\text{-H}}$ = 6.8, 4H, $C\underline{H}Me_{IPr}$), 1.97 (s, 6H, CH_3CN), 1.26 and 1.17 (both d, $J_{H\text{-H}}$ = 6.8, 24H, $CH\underline{Me}_{IPr}$). $^{13}C\{^{1}H\}$-APT NMR (100.4 MHz, CD_3CN, 298K): δ 185.3 (dd, $J_{C\text{-P}}$ = 114.6, $J_{C\text{-Rh}}$ = 46.5, Rh-C_{IPr}), 146.1 (s, $C_{q\text{-IPr}}$), 136.4 (s, C_qN), 134.0 (d, $J_{C\text{-P}}$ = 12.3, $CH_{o\text{-PPh}}$), 132.8 (d, $J_{C\text{-P}}$ = 37.1, C_qP), 129.9, 128.7, 125.3, and 124.7 (both s, CH_{Ph}), 124.0 (s, =CHN), 120.0 (q, $J_{C\text{-F}}$ = 320.0, CF_3), 117.0 (s, $CH_3\underline{C}N$), 28.5 (s, $\underline{C}HMe_{IPr}$), 25.2 and 21.9 (both s, $CH\underline{Me}_{IPr}$), 0.3 (s, $\underline{C}H_3CN$). $^{31}P\{^{1}H\}$ NMR (161.8MHz, CD_3CN, 298 K): δ 37.1 (d, $J_{P\text{-Rh}}$ = 120.7).

Preparation of RhCl(IPr)(PCy_3)(CH_3CN) (16). An acetonitrile solution (5 mL) of **1** (100 mg, 0.079 mmol) was treated with PCy_3 (46 mg, 0.172 mmol). After stirring for 30 min at 60 ºC, the solution was evaporated to dryness. Addition of *n*-hexane caused the precipitation of a pale yellow solid which was washed (3 x 3 mL) and dried in vacuo. Yield: 120 mg (89%). Anal.Calcd. for $C_{47}H_{72}N_3ClPRh$: C, 66.53; H, 8.55; N, 4.95. Found: C, 66.37; H, 8.46; N, 5.18. IR (pure solid, cm^{-1}): ν(C≡N) 2255 (W). ^{1}H NMR (400 MHz, CD_3CN, 298 K): δ 7.56 (t, $J_{H\text{-H}}$ = 7.2, 2H, $H_{p\text{-Ph}}$), 7.43

(d, J_{H-H} = 7.2, 4H, $H_{m\text{-}Ph}$), 7.42 (s, 1H, =CHN), 2.84 (sept, J_{H-H} = 6.8, 4H, C<u>H</u>Me_{IPr}), 1.99 (s, 3H, CH_3CN), 1.9-0.9 (m, 18H, Cy), 1.32 and 1.14 (both d, J_{H-H} = 6.8, 24H, CH<u>Me</u>$_{IPr}$). $^{13}C\{^1H\}$-APT NMR (100.4 MHz, CD_3CN, 298K): δ 188.8 (dd, J_{C-P} = 106.9, J_{C-Rh} = 44.3, Rh-C_{IPr}), 146.8 (s, $C_{q\text{-}IPr}$), 137.7 (s, C_qN), 130.7 and 126.1, (both s, CH_{Ph}), 124.6 (s, =CHN), 118.2 (s, $CH_3\underline{C}N$), 33.0 (d, J_{C-P} = 17.1, PCH), 30.3 and 27.7 (both s, CH_2), 29.4 (s, <u>C</u>HMe_{IPr}), 28.5 (d, J_{C-P} = 10.5, PC<u>H</u>CH_2), 26.3 and 22.9 (both s, CH<u>Me</u>$_{IPr}$), 1.75 (s, $\underline{C}H_3CN$). $^{31}P\{^1H\}$ NMR (161.8MHz, CD_3CN, 298 K): δ 34.6 (d, $J_{P\text{-}Rh}$ = 118.8).

Preparation of RhCl(CO)(IPr)(py) (17). A yellow solution of **3a** (100 mg, 0.0785 mmol) in pyridine (10 mL) was bubbled with CO, while it was stirred for 15 min at room temperature. Then, the solution was concentrated to ca. 1 mL and *n*-hexane added to induce the precipitation of an orange solid, which was washed with *n*-hexane (3 x 3 mL) and dried in vacuo. Yield: 84 mg (83%). Anal. Calcd. for $C_{33}H_{41}N_3ClORh$: C, 62.51; H, 6.52; N, 6.63. Found: C, 62.43; H, 6.47; N, 6.77. IR (pure solid, cm^{-1}): ν(C=O) 1948. ^1H NMR (300 MHz, C_6D_6, 298 K): δ 8.60 (d, J_{H-H} = 4.9, 2H, $H_{2\text{-}py}$), 7.4-7.2 (6H, H_{Ph}), 6.85 (s, 2H, =CHN), 6.55 (t, J_{H-H} = 7.6, 1H, $H_{4\text{-}py}$), 6.14 (dd, J_{H-H} = 7.6, 4.9, 2H, $H_{3\text{-}py}$), 3.58 (sept, J_{H-H} = 6.7, 4H, C<u>H</u>Me_{IPr}), 1.78 and 1.25 (both d, J_{H-H} = 6.7, 24H, CH<u>Me</u>$_{IPr}$). $^{13}C\{^1H\}$-APT NMR (75.4 MHz, C_6D_6, 298 K): δ 187.0 (d, J_{C-Rh} = 82.0, CO), 182.3 (d, J_{C-Rh} = 52.3, Rh-C_{IPr}), 153.2 (s, $C_{2\text{-}py}$), 149.8 (s, $C_{q\text{-}IPr}$), 136.9 (s, C_qN), 135.4 (s, $C_{4\text{-}py}$), 129.9 (s, $C_{3\text{-}py}$), 124.2 and 124.0 (both s, $CH_{Ph\text{-}IPr}$), 123.2 (s, =CHN), 28.9 (s, <u>C</u>HMe_{IPr}), 26.3 and 23.1 (both d, CH<u>Me</u>$_{IPr}$).

Preparation of RhCl(IPr)(O_2)(py) (18). A yellow solution of **3a** (247 mg, 0.194 mmol) in toluene (10 mL) was bubbled with O_2 or air, while it was stirred for 10 min at room temperature. Then, the solution was concentrated to ca. 1 mL and *n*-hexane added to induce the precipitation of a green solid, which was washed with *n*-hexane (3 x 3 mL) and dried in vacuo. Yield: 152 mg (70%). Anal.Calcd. for $C_{32}H_{41}ClN_3O_2Rh$: C, 60.24; H, 6.48; N, 6.59. Found: C, 60.12; H, 6.41; N, 6.53. IR (pure solid, cm^{-1}): ν(O-O) 965. ^1H NMR (300 MHz, toluene-d_8, 263 K): δ 8.58 (d, J_{H-H} = 5.3, 2H, $H_{2\text{-}py}$), 7.2-7.0 (6H, $H_{Ph,}$), 6.73 (s, 2H,=CHN), 6.61 (t, J_{H-H} = 6.4, 1H, $H_{4\text{-}py}$), 6.27 (dd, J_{H-H} = 6.4, 5.3, 2H, $H_{3\text{-}py}$), 3.34 (sept, J_{H-H} = 6.4, 4H, C<u>H</u>Me_{IPr}), 1.61 and 1.17 (both d, J_{H-H} = 6.4, 24H, CH<u>Me</u>$_{IPr}$). $^{13}C\{^1H\}$-APT NMR (75.4 MHz, toluene-d_8, 263 K): δ 167.7 (br, Rh-C_{IPr}), 149.5 (s, $C_{2\text{-}py}$), 146.7 (s, $C_{q\text{-}IPr}$), 137.1 (s, C_qN), 136.1 (s, $C_{4\text{-}py}$), 129.7 and 123.4 (both s, $CH_{Ph\text{-}IPr}$), 122.7 (s, $C_{3\text{-}py}$), 28.7 (s, <u>C</u>HMe_{IPr}), 26.3 and 23.0 (both s, CH<u>Me</u>$_{IPr}$).

Preparation of RhCl(IPr)(O_2)(py)$_2$ (19). A green solution of **18** (100 mg, 0.157 mmol) in toluene (10 mL) was treated with pyridine (130 µl, 0.160 mmol) and it was stirred at room temperature for 15 min. Then, the solvent was evaporated to dryness and subsequent addition of *n*-hexane caused the precipitation of a yellow solid which was washed with *n*-hexane (3 x 2 mL) and dried in vacuo. Yield: 88 mg (75%). Anal.Calcd. for $C_{37}H_{46}ClN_4O_2Rh$: C, 61.97; H, 6.47; N, 7.81. Found: C, 62.20; H, 6.48; N, 7.72. IR (pure solid, cm^{-1}): ν(O-O) 879. ^1H NMR (400 MHz, CD_2Cl_2, 298 K): δ 8.59 and 8.23 (both d, J_{H-H} = 5.4, 4H, $H_{2\text{-}py}$),7.28 (t, J_{H-H} = 7.4, 2H, $CH_{p\text{-}Ph\text{-}IPr}$), 7.49 and 7.46 (both t, J_{H-H} = 7.7, 2H, $H_{4\text{-}py}$), 7.13 (d, J_{H-H} = 7.4, 4H, $CH_{m\text{-}Ph\text{-}IPr}$), 7.06 (s, 2H, =CHN), 7.02 and 6.94 (both dd, J_{H-H} = 7.6, 4.9, 4H, $H_{3\text{-}py}$), 3.17 (sept, J_{H-H} = 6.7, 4H, C<u>H</u>Me_{Ipr}), 1.40 and 1.10 (both d, J_{H-H} = 6.7, 24H, CH<u>Me</u>$_{IPr}$) $^{13}C\{^1H\}$-APT NMR (100.6 MHz, CD_2Cl_2, 298 K): δ 162.4 (d, J_{C-Rh} = 52.09, Rh-C_{IPr}), 153.0 and 149.5 (both s, $C_{2\text{-}py}$), 146.6 (s, $C_{q\text{-}IPr}$), 137.5 (s, C_qN), 136.3 and 135.6 (both s, $C_{4\text{-}py}$), 129.2 and 123.0 (both s, $CH_{Ph\text{-}IPr}$), 125.9 (s, =CHN), 123.0 and 123.8 (s, $C_{3\text{-}py}$), 28.6 (s, <u>C</u>HMe_{IPr}), 26.0 and 22.5 (both d, CH<u>Me</u>$_{IPr}$).

Crystal Structure Determination. Single crystals for the X-ray diffraction studies were grown by slow diffusion of *n*-hexane into toluene (**8**, **18**, **19**) or benzene (**12**) solutions of the complexes. X-ray diffraction data were collected at 100(2) K on a Bruker APEX DUO (**8**, **18**, **19**) or SMART APEX (**12**) CCD diffractometers with graphite-monochromated Mo-Kα radiation (λ = 0.71073 Å) using narrow ω rotations(0.3°). Intensities were integrated and corrected for absorption effects with SAINT-PLUS,[30] and SADABS[31] programs, both included in APEX2 package. The structures were solved by Patterson methods with SHELXS-97[32] and refined, by full matrix least-squares on F^2, with SHELXL-97.[33] All the structures were refined first with isotropic and later with anisotropic displacement parameters for non-disordered non-H atoms. Specific relevant details on each structure are described below. CCDC 1035865-1035868 contain the supplementary crystallographic data for this paper.

Crystal data for **8**: $C_{42}H_{56}ClN_4Rh \cdot 0.5\ C_6H_{14}$; M = 798.39; orange prism 0.222 × 0.163 × 0.108 mm^3; monoclinic, $P2_1/c$; a = 10.1831(4), b = 20.6299(9), c = 19.8046(9) Å, β = 91.3730(10)°; Z = 4; V = 4159.3(3) $Å^3$; D_c = 1.275 $g\cdot cm^{-3}$; μ = 0.510 mm^{-1}; min. and max. absorption correction factors 0.834 and 0.939; $2\theta_{max}$ = 61.10°; 48965 reflections collected, 11930 unique (R_{int} = 0.0446); number of data/restraints/parameters 11930/0/704; final GOF 1.018; R_1 = 0.0353 (9367 reflections, $I > 2\sigma(I)$); w$R(F^2)$ = 0.0875 for all data. Two atoms in the coe ligand were observed disordered; a disorder model with two positions (0.759 and 0.241(8) occupancies) was established. Half a molecule of hexane has also been observed in the asymmetric unit. All hydrogen atoms have been observed and freely refined, except those of the solvent molecule and of the disordered atoms which were included in calculated positions and refined with a positional and thermal riding model.

Crystal data for **12**: $C_{50}H_{56}ClN_3PRh \cdot\ 1.5\ C_6H_6$; M = 985.47; orange prism 0.341 × 0.222 × 0.119 mm^3; triclinic, P-1; a = 11.6031(8), b = 12.7696(9), c = 17.4596(12) Å, α = 79.8850(8), β = 78.2321(8), γ = 80.9152(8)°; Z = 2; V = 2473.1(3) $Å^3$; D_c = 1.323 $g\cdot cm^{-3}$; μ = 0.474 mm^{-1}; min. and max. absorption correction factors 0.855 and 0.946; $2\theta_{max}$ = 57.10°; 28870 reflections collected, 11338 unique (R_{int} = 0.0231); number of data/restraints/parameters 11338/0/594; final GOF 1.076; R_1 = 0.0345 (10165 reflections, $I > 2\sigma(I)$); w$R(F^2)$ = 0.0806 for all data. Two solvent benzene molecules were observed in the crystal structure, the second located around a center of symmetry. Hydrogens were included in calculated positions with riding parameters.

Crystal data for 1**8**: $C_{32}H_{41}ClN_3O_2Rh$; M = 638.06; yellow prism 0.142 × 0.065 × 0.050 mm^3; orthorhombic, *Pnma*; a = 17.4494(10), b = 17.1900(10), c = 10.1596(6) Å; Z = 4; V = 3047.4(3) $Å^3$; D_c = 1.391 $g\cdot cm^{-3}$; μ = 0.681 mm^{-1}; min. and max. absorption correction factors 0.857 and 0.957; $2\theta_{max}$ = 61.08°; 34652 reflections collected, 4620 unique (R_{int} = 0.0652); number of data/restraints/parameters 4620/6/296; final GOF 1.024; R_1 = 0.0348 (2699 reflections, $I > 2\sigma(I)$); w$R(F^2)$ = 0.0861 for all data. A disorder involving the chloride and the oxygen molecule was detected; eventually two positions, at both sides of the metal, were considered for each ligand (0.616 and 0.384(6) occupancies). All hydrogens were observed in the Fourier maps and refined as free isotropic atoms.

Crystal data for **19**: $C_{37}H_{46}ClN_4O_2Rh \cdot 1.5\ C_7H_8$; M = 855.34; orange prism 0.216 × 0.117 × 0.045 mm^3; triclinic; P-1; a = 10.1915(9), b = 12.3169(10), c = 18.8266(16) Å, α = 76.3110(10), β = 82.8450(10), γ = 66.7150(10)°; Z = 2; V = 2107.8(3) Å^3; D_c = 1.348 g·cm^{-3}; μ = 0.512 mm^{-1}; min. and max. absorption correction factors 0.897 and 0.977; $2\theta_{max}$ = 59.28°; 23523 reflections collected, 10755 unique (R_{int} = 0.0305); number of data/restraints/parameters 10755/0/478; final GOF 1.081; R_1 = 0.0331 (9398 reflections, $I > 2\sigma(I)$); w$R(F^2)$ = 0.0831 for all data. Hydrogens were included in calculated positions and refined with a common riding model. A clear toluene solvent molecule was observed in the crystal structure, its constrained hydrogen atoms were also included in the structure. At this stage, six intense residuals were observed around a center of symmetry; its planar disposition, together with their relative electron density, suggested and additional highly disordered half molecule of toluene (SQUEEZE evaluation: void of 177 Å^3, electron density of 56 e$^-$). Eventually, the contribution of this disordered molecule was extracted from the structure factor list using SQUEEZE program.[34]

Computational details. All calculations were performed with the Gaussian09 package[35] at the M06 level.[36] Rhodium was represented by the relativistic effective core potential (RECP) from the Stuttgart group and the associated basis set (SDD keyword in Gaussian 09).[37] The 6-31G(d) basis set was used for all the other atoms.[38] Full optimizations of geometry without any constraint were performed, followed by analytical computation of the Hessian matrix to confirm the nature of the stationary points as minima on the potential energy surface. In the Table XX we have reported the computational results including the cartesian coordinates (in Å), absolute energy (in a.u) and graphical representation including selected geometrical parameters. Charge decomposition analysis (CDA) have been performed using Dapprich and Frenking's CDA 2.2 program[39] using the same methods as in the Gaussian calculations.

Determination of rotational barriers. Full line-shape analysis of the dynamic ^{1}H NMR spectra of **17, 18** and **19** were carried out using the program gNMR (Cherwell Scientific Publishing Limited). The transverse relaxation time, T_2, was estimated at the lowest temperature. Activation parameters $\Delta H^{\ddagger}$ and $\Delta S^{\ddagger}$ were obtained by linear least-squares fit of the Eyring plot. Errors were computed by published methods.[40]

Address

‡*Departamento de Química Inórganica-Instituto de Síntesis Química y Catálisis Homogénea (ISQCH), Universidad de Zaragoza-CSIC, C/ Pedro Cerbuna 12, Zaragoza, 50009, Spain.*
E-mail: rcastar@unizar.es
† *Center for Refining & Petrochemicals King Fahd University of Petroleum & Minerals, Dhahran, 31261, Saudi Arabia.*

Electronic Supplementary Information (ESI) available: Cartesian coordinates and energy values for DFT calculated complexes. CCDC 1035865-1035868.

References

1 (*a*) K. M. Engle, D.-H. Wang, J.-Q. Yu, *J. Am. Chem. Soc.* 2010, **132**, 14137; (*b*) I. D. Gridnev, M. Watanabe, H. Huang, T. Ikariya, T. *J. Am. Chem. Soc.* 2010, **132**, 16637; (*c*) B. Gnanaprakasan, J. Zhang, D. Milstein, *Angew. Chem. Int. Ed.* 2010, **49**, 1468; (*d*) C. González-Rodríguez, R. J. Pawley, A. B. Chaplin, A. N. Thompson, A. S. Weller, M. C. Willis, *Angew. Chem. Int. Ed.* 2011, **50**, 5134; (*e*) S. T. Madrahimov, J. F. Hartwig, *J. Am. Chem. Soc.* 2012, **134**, 8136; (*f*) B. K. Keitz, K. Endo, P. R. Patel, M. B. Herbert, R. H. Grubbs, *J. Am. Chem. Soc.* 2012, **134**, 8136; (*g*) H. Teller, M. Corbet, L. Mantilli, G. Gopukumar, R. Goddard, W. Thiel, A. Fürstner, *J. Am. Chem. Soc.* 2012, **134**, 15331; (h) I. A. Sanhueza, A. M. Wagner, M. S. Sanford, F. Schoenebeck, *Chem. Sci.* 2013, **4**, 2767; (i) R. K. M. Khan, S. Torker, A. M. Hoveyda *J. Am. Chem. Soc.* 2014, **136**, 14337.

2 (*a*) C. J. Elsevier, J. Reedijk, P. H. Walton, M. D. Ward, *Dalton Trans.* 2003, 1869; (*b*) R. H. Crabtree, *New J. Chem.* 2011, **35**, 18; (*c*) A. L. Noffke, A. Habtemariam, A. M. Pizarro, P. J. Sadler, *Chem. Commun.* 2012, **48**, 5219.

3 (*a*) W. A. Herrmann, *Angew. Chem. Int. Ed.* 2002, **41**, 1290; (*b*) E. A. B. Kantchev, C. J. O´Brien, M. G. Organ, *Angew. Chem. Int. Ed.* 2007, **46**, 2768; (*c*) J. M. Praetorius, C. M. Crudden, *Dalton Trans.* 2008, 4079; (*d*) A. J. Arduengo III, L. I. Iconaru, *Dalton Trans.* 2009, 6903; (*e*) O. Schuster, L. Yang, H. G. Raubenheimer, M. Albrecht *Chem. Rev.* 2009, **109**, 3445; (*f*) S. Díez-González, N. Marion, S. P. Nolan, *Chem. Rev.* 2009, **109**, 3612; (*g*) R. Visbal, M. C. Gimeno, *Chem. Soc. Rev.* 2014, **43**, 3551; (h) M. N. Hopkinson, C. Richter, M. Schedler F. Glorius, *Nature* 2014, **510**, 485; (i) J. A. Mata, F. E. Hahn, E. Peris, *Chem. Sci.* 2014, **5**, 1723.

4 (*a*) X. Hu, Y. Tang, P. Gantzel, K. Meyer, *Organometallics* 2003, **22**, 612; (*b*) D. Nemcsok, K. Wichmann, G. Frenking, *Organometallics* 2004, **23**, 3640; (c) L. Mercs, G. Labat, A. Neels, A. Ehlers, M. Albrecht, *Organometallics* 2006, **25**, 5648; (*d*) D. M. Khramov, V. M. Lynch, C. W. Bielawski, *Organometallics* 2007, **26**, 6042; (*e*) H. Jacobsen, A. Correa, A. Poater, C. Costabile, L. Cavallo, *Coord. Chem. Rev.* 2009, **253**, 687; (*f*) A. Comas-Vives, J. N. Harvey, *Eur. J. Inorg. Chem.* 2011, 5025; (g) M. Alcarazo, *Dalton Trans*. 2011, **40**, 1839; (h) D. J. Nelson, S. P. Nolan *Chem. Soc. Rev.* 2013, **42**, 6723.

5 (*a*) S. Würtz, F. Glorius, *Acc. Chem. Res.* 2008, **41**, 1523; (*b*) A. R. Chianese, A. Mo, D. Datta, *Organometallics* 2009, **28**, 465; (*c*) H. Clavier, S. P. Nolan, *Chem. Commun.* 2010, **46**, 841; (*d*) B. R. Dible, R. E. Cowley, P. L. Holland, *Organometallics* 2011, **30**, 5123; (*e*), M. Teci, E. Brenner, D. Matt, L. Toupet, *Eur. J. Inorg. Chem.* 2013, 2841; (f) S. Dierick, D. F. Dewez, I. E. Markó, *Organometallics* 2014, **33**, 677; (g) N. Phillips, R. Tirfoin, S. Aldridge *Chem. Eur. J.* 2014, **20**, 3825.

6 A. Di Giuseppe, R. Castarlenas, J. J. Pérez-Torrente, M. Crucianelli, V. Polo, R. Sancho, F. J. Lahoz, L. A. Oro, *J. Am. Chem. Soc.* 2012, **134**, 8171.

7 (*a*) I. P. Beletskaya, V. P. Ananikov, *Chem. Rev.* 2011, **111**, 1596; (*b*) R. Castarlenas, A. Di Giuseppe, J. J. Pérez-Torrente, L. A. Oro, *Angew. Chem. Int. Ed.* 2013, **52**, 213.

8 (*a*) D. J. Berrisford, C. Bolm, K. B. Sharpless, *Angew. Chem. Int. Ed. Engl.* 1995, **34**, 1059; (*b*) C. C. Romão, F. E. Kühn, W. A. Herrmann, *Chem. Rev.* 1997, **97**, 3197; (*c*) E. M. Vogl, H. Gröger, M. Shibasaki *Angew. Chem. Int. Ed.* 1999, **38**, 1570; (*d*) T. Nishimura, T. Onoue, K. Ohe, S. Uemura, *J. Org. Chem.* 1999, **64**, 6750; (*e*) E. M. Ferreira, B. M. Stoltz, *J. Am. Chem. Soc.* 2003, **125**, 9578; (*f*) I. Kamiya, E. Nishinaka, A. Ogawa, *J. Org. Chem.* 2005, **70**, 696; (*g*) J. Nasielski, N. Hadei, G. Achonduh, E. A. B. Kantchev, C. J. O´Brien, A. Lough, M. G. Organ, *Chem. Eur. J.* 2010, **16**, 10844; (*h*) A. J. Pardey, C. Longo, *Coord. Chem. Rev.* 2010, **254**, 254; (*i*) S. R. Neufeldt, M. S. Sanford, *Acc. Chem. Res.* 2012, **45**, 936; (*j*) M. D. Kärkäs, T. Åkermark, H. Chen, J. Sun, B. Åkermark, *Angew. Chem. Int. Ed.* 2013, **52**, 4189.

9 A NMR tube charged with 0.005 mmol of [Rh(μ-Cl)(η^2-coe)(IPr)]$_2$ were treated with 0.1 mmol of CH_3CN, 0.5 mmol of tiophenol and 0.5 mmol of phenylacetylene. After 16 h at room temperature a ratio 56:44 branched/linear vinyl sulfide were obtained.

10 (*a*) L. Mercs, A. Neels, H. Stoeckli-Evans, M. Albrecht, *Dalton Trans.* 2009, 7168; (*b*) J. M. Smith., J. R. Long, *Inorg.Chem.* 2010, **49**, 11223; (*c*) C. S. Vogel, F. W. Heinemann, M. M. Kushniyarov, K. Meyer, *Inorg.Chim. Acta* 2010, **364**, 226.

11 (*a*) P. de Frémont, N. Marion, S. P. Nolan, *J. Organomet. Chem.* 2009, **694**, 551; (*b*) C. C. Ho, S. Chatterjee, T.-L. Wu, K.-T. Chang, T.-H. Hsiao, H. M. Lee, *Organometallics* 2009, **28**, 2837; (*c*) W. W.

N. O, A. J. Lough, R. H. Morris, *Chem. Commun.* 2010, 8240. (*d*) J. C. Bernhammer, H. V. Huynh, *Organometallics* 2012, **31**, 5121.

12 (*a*) X.-Y. Yu, B. O. Patrick, B. R. James, *Organometallics* 2006, **25**, 4870; (*b*) X.-Y. Yu, H. Sun, B. O. Patrick, B. R. James, *Eur. J. Inorg. Chem.* 2009, 1752; (*c*) A. Di Giuseppe, R. Castarlenas, J. J. Pérez-Torrente, F. J. Lahoz, V. Polo, L. A. Oro, *Angew. Chem. Int. Ed.* 2011, **50**, 3938; (*d*) O. V. Zenkina, E. C. Keske, R. Wang, C. M. Crudden, *Angew. Chem. Int. Ed.* 2011, **50**, 8100; (*e*) O. V. Zenkina, E. C. Keske, R. Wang, C. M. Crudden, *Organometallics* 2011, **30**, 6423; (*f*) O. V. Zenkina, E. C. Keske, G. S. Kochhar, R. Wang, C. M. Crudden, *Dalton Trans.* 2013, **42**, 2282; (*g*) R. Azpíroz, A. Di Giuseppe, R. Castarlenas, J. J. Pérez-Torrente, L. A. Oro, *Chem. Eur. J.* 2013, **19**, 3812; (*h*) L. Palacios, A. Di Giuseppe, A. Opalinska R. Castarlenas, J. J. Pérez-Torrente, F. J. Lahoz, L. A. Oro, *Organometallics* 2013, **32**, 2768; (*i*) L. Rubio-Pérez, R. Azpíroz, A. Di Giuseppe, V. Polo, R. Castarlenas, J. J. Pérez-Torrente, L. A. Oro *Chem. Eur. J.* 2013, **19**, 15304; (*j*) L. Palacios, M. J. Artigas; V. Polo, F. J. Lahoz, R. Castarlenas, J. J. Pérez-Torrente, L. A. Oro, *ACS Catal.* 2013*,* **3***,* 2910; (*k*) A. Di Giuseppe, R. Castarlenas, J. J. Pérez-Torrente, F. J. Lahoz, L. A. Oro, *Chem. Eur. J.* 2014, **20**, 8391; (*l*) R. Azpíroz, L. Rubio-Pérez, A. Di Giuseppe, V. Passarelli, F. J. Lahoz, R. Castarlenas, J. J. Pérez-Torrente, L. A. Oro, *ACS Catal*. 2014, **4**, 4244.

13 C. E. Willans, K. M. Anderson, M. J. Paterson, P. C. Junk, L. J. Barbour, J. W. Steed, *Eur. J. Inor. Chem.* 2009, 2835.

14 (*a*) P. H. M. Budzelaar, M. M. P. Moonen, R. de Gelder, J. M. M. Smits, A. W. Gal, *Eur. J. Inor. Chem.* 2000, 753. (*b*) G. Canepa, C. D. Brandt, H. Werner, *J. Am. Chem. Soc.* 2002, **124**, 9666.

15 (*a*) A. R. Chianese, X. Li, M. C. Janzen, J. W. Faller, R. H. Crabtree, *Organometallics* 2003, **22**, 1663; (*b*) S. Burling, S. Douglas, M. F. Mahon, D. Nama, P. S. Pregosin, M. K. Whittlesey, *Organometallics* 2006, **25**, 2642; (*c*) V. Ritleng, C. Barth, E.. Brenner, S. Milosevic, S., M. J. Chetcuti, *Organometallics* 2008, **42**, 4223; (*d*) M. M. Gallagher, A. D. Rooney, J. J. Rooney, *J. Organomet. Chem.* 2008, **693**, 1252; (*e*) S. Leuthäuβer, V. Schmidts, C. M. Thiele, H. Plenio, *Chem. Eur. J.* 2008, **14**, 5465; (*f*) C. L. Vélez, P. R. L. Markwick, R. L. Holland, A. G. DiPasquale, A. L. Rheingold, J. M. O'Connor, *Organometallics* 2010, **29,** 6695; (*g*) F. Ragone, A. Poater, L. Cavallo, *J. Am. Chem. Soc.* 2010, **132**, 4249; (*h*) L. Busetto, M. C. Cassani, C. Femoni, M. Mancinelli, A. Mazzanti, R. Mazzoni, G. Solinas, *Organometallics* 2011, **30**, 5258; (*i*) L. Palacios, X. Miao, A. Di Giuseppe, S. Pascal, C. Cunchillos, R. Castarlenas, J. J. Pérez-Torrente, F. J. Lahoz, P. H. Dixneuf, L. A. Oro, *Organometallics* 2011, **30**, 5208.

16 T. T. To, C. E. Barnes, T. J. Burkey, *Organometallics,* 2004, **23**, 2708.

17 (a) B. T. Heaton, J. A. Iggo, C. Jacob, J. Nadarajah, M. A. Fontaine, R. Messere, A. F. Noels, *J. Chem. Soc., Dalton Trans.* 1994, 2875; (*b*) L. Carlton, *Magn. Reson. Chem.* 2004, **42**, 760; (*c*) S. P. Reade, D. Nama, M. F. Mahon, P. S. Pregosin, M. K. Whittlesey, *Organometallics* 2007, **26**, 3484.

18 For an example of Rh^{I}-pyridine square-planar complex with mutually *cis* PPh_3 see: P. Marcé, C. Godard, M. Feliz, X. Yáñez, C. Bo, S. Castillón, *Organometallics* 2009, **28**, 2976.

19 For an example of a square-planar complex with phosphine and pyridine *cis* to NHC see: N. Tsoureas, A. A. Danopoulos, A. A. D. Tulloch, M. E. Light, *Organometallics,* 2003, **22**, 4750.

20 T. Leyssens, D. Peeters, A. G. Orpen, J. N. Harvey, *Organometallics,* 2007, **26**, 2637.

21 M. V. Baker, D. H. Brown, R. A. Haque, P. V. Simpson, B. W. Skelton, A. H. White, C. C. Williams, *Organometallics,* 2009, **28**, 3793.

22 (*a*) B. Çetinkaya, P. B. Hitchcock, M. F. Lappert, D. B. Shaw, K. Spyropoulos, N. J. V. Warhurst, *J. Organomet. Chem.* 1993, **459**, 311; (*b*) W. A. Herrmann, J. Fischer, K. Öfele, G. R. J. Artus, *J. Organomet. Chem.* 1997, **530**, 259; (*c*) J. M. Praetorius, R. Wang, C. M. Crudden, *Eur. J. Inorg. Chem.* 2009, 1746.

23 E. C. Keske, O. V. Zenkina, A. Asadi, H. Sun, J. M. Praetorius, D. P. Allen, D. Covelli, B. O. Patrick, R. Wang, P. Kennepohl, B. R. James, C. M. Crudden, *Dalton Trans.* 2013, **42**, 7414.

24 (*a*) J. M. Praetorius, D. P. Allen, R. Wang, J. D. Webb, F. Grein, P. Kennepohl, C. M. Crudden, *J. Am. Chem. Soc.* 2008, **130**, 3724; (*b*) C. M. Frech, L. J. W. Shimon, D. Milstein, *Helv. Chim. Acta* 2006, **89**, 1730; (*c*) A. Y. Verat, H. Fan, M. Pink, Y. S. Chen, K. G. Caulton, *Chem. Eur. J.* 2008, **14**, 7680.

25 (*a*) Y. Takahashi, M. Hashimoto, S. Hikichi, M. Akita, Y. Moro-Oka, *Angew. Chem. Int. Ed.* **1999**, *38*, 3074; (*b*) M. Ahijado, T. Braun, D. Noveski, N. Kocher, B. Neumann, D. Stalke, H.-G. Stammler, *Angew. Chem. Int. Ed.* **2005**, *44*, 6947; (*c*) G. Meier, T. Braun, *Angew. Chem. Int. Ed.* **2011**, *50*, 3280; (*d*) J. Cipot-Wechsler, D. Covelli, J. M. Praetorius, N. Hearns, O. V. Zenkina, E. C. Keske, R. Wang, P. Kennepohl, C. M. Crudden, *Organometallics* **2012**, *31*, 7306.

26 (*a*) C. D. Abernethy, G. M. Codd, M. D. Spicer, M. K. Taylor, *J. Am. Chem. Soc.* 2003, **125**, 1128; (*b*) K. Miqueu, E. Despagnet-Ayoub, P. W. Dyer, D. Bourissou, G. Bertrand, *Chem. Eur. J.* 2003, **9**, 5858; (*c*) B. M. Gardner, J. McMaster, S. T. Liddle, *Dalton Trans*. 2009, 6924; (*d*) B.-L. Lin, P. Kang, T. D. P. Stack, *Organometallics,* 2010, **29**, 3683.

27 S. Dapprich, G. Frenking, *J. Phys. Chem.*, 1995, **99**, 9352.

28 (*a*) G. Frenking, K. Wichmann, N. Fröhlich, C. Loschen, M. Lein, J. Frunzke, V. M. Rayón, *Coord. Chem. Rev.* 2003, **238–239**, 55; (*b*) P. Parameswaran, G. Frenking, *Chem. Eur. J.* 2009, **35**, 8807; (*c*) Y. Tulchinsky, M. A. Iron, M. Botoshansky and M. Gandelman, *Nat. Chem.* 2011, **3**, 525. (*d*) A. C. Tsipis, G. N. Gkekas, *Dalton Trans*. 2013, **42**, 8307.

29 J. S. Dewar, *Bull. Soc. Chim. Fr.* 1951, **18**, c79; (*b*) J. Chatt, L. A. Duncanson, *J. Chem. Soc.* 1953, 2939.

30 *SAINT-PLUS, version 6.01*, Bruker AXS, Inc., Madison, USA, 2001.

31 G. M. Sheldrick, *SADABS*, University of Göttingen, Göttingen, Germany, 1999.

32 (a) G. M. Sheldrick, *Acta Crystallogr., Sect. A: Fundam. Crystallogr.*, 1990, **46**, 467–473; (b) G. M. Sheldrick, *Methods Enzymol.*, 1997, **276**, 628–641.

33 G. M. Sheldrick, *Acta Crystallogr., Sect. A: Fundam. Crystallogr.*, 2008, **64**, 112–122.

34 *SQUEEZE Program*, P. v.d. Sluis, A. L. Spek, *Acta Crystallogr., Sect A: Fundam. Crystallogr.*, 1990, **46**, 194-201.

35 Gaussian 09, Revision A.1, M. J. Frisch, G. W. Trucks, H. B. Schlegel, G. E. Scuseria, M. A. Robb, J. R. Cheeseman, G. Scalmani, V. Barone, B. Mennucci, G. A. Petersson, H. Nakatsuji, M. Caricato, X. Li, H. P. Hratchian, A. F. Izmaylov, J. Bloino, G. Zheng, J. L. Sonnenberg, M. Hada, M. Ehara, K. Toyota, R. Fukuda, J. Hasegawa, M. Ishida, T. Nakajima, Y. Honda, O. Kitao, H. Nakai, T. Vreven, J. A. Montgomery, Jr., J. E. Peralta, F. Ogliaro, M. Bearpark, J. J. Heyd, E. Brothers, K. N. Kudin, V. N. Staroverov, R. Kobayashi, J. Normand, K. Raghavachari, A. Rendell, J. C. Burant, S. S. Iyengar, J. Tomasi, M. Cossi, N. Rega, J. M. Millam, M. Klene, J. E. Knox, J. B. Cross, V. Bakken, C. Adamo, J. Jaramillo, R. Gomperts, R. E. Stratmann, O. Yazyev, A. J. Austin, R. Cammi, C. Pomelli, J. W. Ochterski, R. L. Martin, K. Morokuma, V. G. Zakrzewski, G. A. Voth, P. Salvador, J. J. Dannenberg, S. Dapprich, A. D. Daniels, Ö. Farkas, J. B. Foresman, J. V. Ortiz, J. Cioslowski, and D. J. Fox, Gaussian, Inc., Wallingford CT, 2009.

36 Y. Zhao, D. G. Truhlar, *Theor. Chem. Acc.* 2008, **120**, 215.

37 D. Andrae, U. Haeussermann, M. Dolg, H. Stoll, H. Preuss, *Theor. Chim. Acta* 1990, **77**, 123.

38 P. C. Hariharan, J. A. Pople, *Theor. Chim. Acta* 1973, **28**, 213.

39 CDA 2.2, S. Dapprich, G. Frenking, M. von Hopffgarten, Philipps-Universität Marburg, **2013**. This program is free avaible: http://www.uni-marburg.de/fb15/ag-frenking/cda_g03g09.

40 P. M. Morse, M. O. Spencer, S. R. Wilson, G. S. Girolami, *Organometallics* 1994, **13**, 1646.